Article

Not peer-reviewed version

Bridging Archaeology and Marine Ecology: Coral Archives of Hellenistic Coastal Change

Tali Mass *, Jeana Drake, Stephane Martinez, Jarosław Stolarski, Jacob Sharvit

Posted Date: 17 July 2025

doi: 10.20944/preprints202507.1343.v1

Keywords: archaeological corals; scleractinia; mediterranean sea; Akko port; photophysiology; nitrogen source; ancient DNA

 doi:10.20944/preprints202507.1343.v1

Article

Bridging Archaeology and Marine Ecology: Coral Archives of Hellenistic Coastal Change

Tali Mass [1,2,*], Jeana Drake [3], Stephane Martinez [1], Jarosław Stolarski [4] and Jacob Sharvit [5]

[1] Department of Marine Biology, Leon H. Charney School of Marine Sciences, University of Haifa, Haifa, Israel
[2] Morris Kahn Marine Research Station, Leon H. Charney School of Marine Sciences, University of Haifa, Sdot Yam, Israel
[3] Earth, Planetary, and Space Sciences, University of California, Los Angeles, USA
[4] Institute of Paleobiology, Polish Academy of Sciences, Warsaw, Poland
[5] Israel Antiquities Authority, Marine Archaeology Unit, Jerusalem, Israel
* Correspondence: tmass@univ.haifa.ac.il

Abstract

Stony corals are long-lived, calcifying cnidarians that provide critical records of past coastal environmental conditions. This study analyzes sub-fossil *Cladocora* sp. colonies from ancient Akko, Israel, dated to the Hellenistic period (~335–94 BCE), alongside modern *Cladocora caespitosa* from Haifa Bay. The sub-fossil corals, preserved within archaeological strata, offer insights into past seawater conditions, anthropogenic influences, and harbor dynamics. We employ micromorphology, stable isotope analysis, and DNA sequencing to assess species identity, colony growth form, and environmental conditions experienced by the corals. Comparisons suggest that Hellenistic Akko corals grew in high-light, cooler-water, high-energy environments, potentially with exposure to terrestrial waste. The exceptional preservation of these colonies indicates rapid burial, possibly linked to ancient harbor activities or extreme sedimentation. Our results demonstrate the utility of scleractinian corals as valuable paleoenvironmental archives, capable of integrating both biological and geochemical proxies to reconstruct past marine conditions. By linking archaeological and ecological records, this approach offers a more comprehensive understanding of long-term human-environment interactions in coastal areas. This multidisciplinary approach enhances our understanding of historical coastal dynamics, ancient harbor use, climate variability, and anthropogenic impacts.

Keywords: Archaeological corals; Scleractinia; Mediterranean Sea; Akko port; photophysiology; nitrogen source; ancient DNA

1. Introduction

Stony corals are calcifying cnidarians that are responsible for the formation of large, shallow-water, coastal reef ecosystems [1,2] that house ~25% of described marine fishes and invertebrates [3,4]. They have adapted to thrive across relatively large gradients of environmental/abiotic factors including temperature, turbidity, flow, light and nutrient availability [5]. At the species level, stony corals exhibit abundant examples of phenotypic plasticity, or visible responses to environmental factors despite shared genotypes. Plasticity of coral growth location, morphology, physiology, and gene expression has been documented in response to light [6–9], water flow [10,11], nutrient availability [12], and seawater chemistry [13], and aims to maintain energy acquisition across environmental gradients. As such, stony corals have persisted, as a taxonomic order (Scleractinia), for more than 240 million years, enduring multiple catastrophes in Earth's history [14], and leaving them as records of not only fairly static environmental growth conditions over the long term (e.g.,

 doi:10.20944/preprints202507.1343.v1

presence/absence, macromorphology, and bulk skeleton analysis) but also of decadal, seasonal, and impending terminal ecosystem changes. For instance, it has been well-documented that the trace element and stable isotope composition of scleractinian coral skeletons records environmental signals from the surrounding seawater in species-specific ways review by [15], allowing paleoceanographic reconstructions of seawater temperature, cation concentrations, and pH [16,17] Recently Gothmann et al. [18] extended the use of fossil corals as geochemical archives into the Mesozoic. In addition, the symbiotic relationship between scleractinian corals and photosynthetic dinoflagellates can be detected from the isotopic composition of organic matter embedded within the coral skeleton (SOM), which reflects photosymbiotic activity (and hence light conditions) [19–21]. This isotopic signatures also provide insights into the relative contributions of auto- versus heterotrophy to both fixed carbon and nitrogen nutritional sources [19,20,22–24]. Multiple lines of evidence suggest that the nitrogen isotopic composition ($\delta^{15}N$) of corals' SOM and other calcifying organisms can remain stable over geological timescales [19,22,25–28]. As such, coral-bound $\delta^{15}N$ serves as a robust proxy for assessing photosymbiotic status in fossil corals [19,22], with well-preserved aragonitic skeletons retaining these isotopic signatures for over 200 million years following the death of the holobiont (the coral host and its associated symbiotic community)[e.g., [22]].

Cladocora caespitosa (Linnaeus, 1767; family Cladocoridae) is a colonial symbiotic stony coral, endemic to the Mediterranean Sea [29]. It is considered a remnant reef-building species and a vital evolutionary link between tropical coral reefs and the ancient reef ecosystems that existed in the Mediterranean prior to the end of the Messinian period [30]. Although large reef structures formed by this coral are frequently observed in the fossil record [30], they have become exceptionally rare in the modern Mediterranean [31,32]. Due to its longevity and distinctive calcification patterns, *C. caespitosa* is increasingly studied as a natural archive for reconstructing past environmental and climatic conditions in the Mediterranean region [33,34].

The Mediterranean of the Hellenistic period (232- 63 BCE) was heavily populated along the coasts [35], with a sea level and sea surface temperatures probably lower and cooler than today, respectively [36]. Recent studies have revealed significant changes in sea surface temperatures (SSTs) in the eastern Mediterranean over the past millennia, recording a warming trend in the region, with the 20th century being the warmest period in the last millennium [36,37]. The Hellenistic period was unstable in the human history of the Syria-Palestine region, withhe "Syrian wars", the longest sequence of wars in the ancient world [38], spanning from 301 BCE or earlier to 103-101 BCE. Modern Akko (also called Acre and known at the time as Ptolemais-Ake; Figure 1) became a Greek polis at the end of the fourth century BCE, and was an important Egyptian military port and city during the "Syrian Wars" [39]. The city became active in regional and maritime trade, and it fairly quickly became one of the most important and prosperous cities in the region. During the Roman period, the harbor was the most important gateway to Europe and Rome and was favored by the Roman troops as the regular landing place for over two centuries [40]. Surveys and reconstructions by the British Mandate Department of Antiquities (1920s - 1940s) revealed and then confirmed the importance of greater Akko to past geopolitical conflicts in the region [41]. Later archaeological surveys and excavations of Akko then began in the mid-1960s [42], revealing a variety of underwater breakwaters, foundations, and shipwrecks. Underwater excavations of coastal Akko in the 2010s under the auspices of the Israeli Antiquities Authority established six archaeological strata from the Hellenistic period (i.e., sub-fossil) to the British Mandate [40,43]. During these underwater excavations eight square (2x2m.) pits were dug among them only three were dug up to the bedrock, in which several well-preserved corals of genus *Cladocora* were identified as colonizers of the ancient bedrock [40,43]. The colonies were and radiocarbon dated to 335-94 BCE [44]. Based on their size, corallite length and known modern growth rates of *Cladocora* [45,46], they were likely decades old at the time of burial. The relatively large colonies and attachment to the bedrock at a depths that have remained shallow (~10 m) over the past two kiloanna; led the authors to suggest that the site was minimally turbid - allowing sufficient sunlight for coral growth - prior to 94 BCE, with subsequent burial following an acute sedimentation event leading to excellent macro- and microscopic skeletal

 doi:10.20944/preprints202507.1343.v1

feature preservation [40,43]. These *Cladocora* corals can thus have the potential to reveal the underwater environment and human uses of the Akko harbor from ~2300 years ago.

In this study, we apply multiple analyses to several shallow sub-fossil *Cladocora* sp. colonies excavated from portions of the Akko port dated to the Hellenistic period as well as to live *Cladocora caespitosa* from 10 and 30 m depth in Haifa Bay (~10 km north and south, respectively, of Akko Bay; Figure 1). Both micromorphology and DNA sequencing (modern and sub-fossil) support taxonomic identification. Colony growth form (macromorphology) and SOM amino acid stable isotope analysis from both modern and sub-fossil specimens suggests that they experienced roughly similar water energy environments and trophic position, although the sub-fossil *Cladocora* appears to have experienced higher light levels, at shallow depths, and exposure to anthropogenic terrestrial waste (i.e., sewage). Further, the very high degree of colony preservation suggests a rapid burial event. By comparing various measurements from genetically similar corals separated by 2,000 years, this study offers a more integrated and comprehensive reconstruction of the eastern Mediterranean's historical physical and social environments than analyses conducted in isolation.

Figure 1. Location of sampling locations along Israel's Mediterranean coast (A). Inset (B) shows, from north to south, Naharia, Akko port excavation site of well-preserved sub-fossil Cladocora, and the southern Haifa Bay Leonid shipwreck.

2. Materials and Methods

2.1. Collection

Modern Specimens: Small fragment (approximately 2 cm each) from five live colonies identified as *Cladocora caespitosa* were collected via SCUBA from the Israeli Mediterranean Sea in January 2021 at 30 m depth in Haifa Bay, Israel, from the Leonid ship wreck (32.86975N 34.95405E) (Figure 1). One fragment was immediately frozen in dry nitrogen for genetic analysis, and the rest were transported on ice and stored in -20 °C until fragmentation for ex situ analyses. Additionally, five newly discovered colonies at a depth of 10 meters on Naharia, ranging in size from 3 to 10 cm in diameter, were examined in situ for photophysiology.

Sub-Fossil Specimens: Five Sub-fossil *Cladocora* sp. colonies were collected via SCUBA diving during the excavation of the Hellenistic-early Roman Harbour of Akko in May-June 2012 and 2014 at 2.5 m depth. Excavation pits 1, 2, and 7 are located at (32.92094N 35.07138E). All excavations were carried out under the auspices of the Israeli Antiquities Authority under permits A6557, A6829, and A7120. Colonies were documented in situ, detached carefully from the bedrock and put together with seawater in a closed plastic box. Boxes were tagged with the following data: permit no., dive and date, pit no. depth; samples of sediments from the surrounding area were taken separately. The coral boxes were transferred to the lab and stored at 4°C until further analysis [43]. The sub-fossil skeletal fragments used for scanning electron microscopy and computed tomography analyses as well as some comparable modern specimens of *Cladocora* are housed at the Institute of Paleobiology, Polish Academy of Sciences (abbreviated ZPAL).

 doi:10.20944/preprints202507.1343.v1

Both modern and sub-fossil corals were collected for subsequent physiological, skeletal, and Compound specific stable isotope analysis of amino acids (CSIA-AA).

2.2. Photosynthetic Parameters Assessment

In situ physiological assays were conducted 20 September 2023 at 10 and 30 m on five *Cladocora* colonies each at 10 m (Naharia, Israel) and 30 m (Leonid shipwreck, Haifa Bay, Israel) depth using a Diving-Fluorescence Induction and Relaxation (FIRe) fluorometer [47], following methods previously described [48]. In brief, to account for intra-colony differences in light exposure, five readings were collected per colony and averaged to reflect the photophysiology of the entire colony in the analysis. As Diving-FIRe is based on a kinetic approach, it offers instantaneous measurements of ETR_{max} without dark adaptation of the sample, therefore allowing in-situ measurements during the daytime. Photophysiology data were determined to display normal distribution and homogenous variance between depths so that parametric statistical tests were applied.

2.3. Skeletal Morphology

2.3.1. Scanning electron Microscopy

Modern coral fragments were airbrushed and then submerged in 3% sodium hypochlorite for one hour to remove any remaining tissue, rinsed in freshwater, and dried at 60°C. Sub-fossil coral fragments were sonicated in deionized water three times for five minutes each to remove debris and loosely cemented sand and then dried at 60°C. Skeletal micro-morphology was visualised using a Thermo Fisher (Philips) XL20 scanning electron microscope (SEM) at the Institute of Paleobiology, Polish Academy of Sciences. All samples were sputter coated with platinum and photographed. SEM was also used to visualize the micro-structural features of polished sections that were lightly etched in Mutvei's solution following Schöne et al., [49].

2.3.2. Computed Tomography Scanning

3D visualization of the internal structure of the coralla was made with a Zeiss XRadia MicroXCT-200 system at the Institute of Paleobiology, Polish Academy of Sciences. Scans were performed using the following parameters: voltage: 60 kV, power: 10 W, exposure time: 6 s, pixel size: 19.47 µm, 1201 projections. Three-dimensional images were obtained by processing with the AVIZO7.1 Fire Edition software.

2.4. DNA Extraction

2.4.1. Modern Corals

Five sub-samples of modern *C. caespitosa* genomic DNA were extracted using the Wizard Genomic DNA Purification Kit (Promega, USA). PCR amplifications were performed using Kodaq 2X PCR MasterMix (ABM, Richmond, BC Canada) [50]. To verify coral and photosymbiont taxonomy, we queried the highly conserved cytochrome oxidase subunit 1 (COI) using the following primers—FOL-LDEG (forward) 5′-TCWACHAAY CAT AAR GAY ATWGG-3′ and FOL-HDEG (reverse) 5′-TCWACHAAY CAT AAR GAY ATWGG-3′ (modified from [51]). In addition, the internal transcribed spacer (ITS2) region of Symbiodiniaceae rDNA was amplified using Symbiodiniaceae-specific

primers CS1F (forward) 5′-ACA CTG ACG ACA TGG TTC TAC ATG TGA ATT GCA GAA CTC CGT G-3′ and CS2R (reverse) 5′-TAC GGT AGC AGA GAC TTG GTC TTA CTT ATA TGC TTA AAT TCR GCGG-3′ taken from [52], respectively (Table S1). The host COI region was sequenced by the Sanger sequencing method using the ABI 3730xl DNA Analyser while Symbiodiniaceae ITS2 was sequenced on the Illumina Miseq using a v2-500 cycle kit to generate 250x 2, paired-end reads. COI sequences from the five samples were aligned using ClustalW to create a consensus sequence, which was BLASTed in NCBI's GeneBank for species identification. Symbiodiniaceae ITS2 data were

 doi:10.20944/preprints202507.1343.v1

demultiplexed by the Illumina software, and the paired forward and reverse fastq.gz files were submitted to SymPortal [53] to assess the diversity and relative abundance of symbiont species within each sample.

2.4.2. Sub-Fossil Corals

Excavated sub-fossil Hellenistic *Cladocora* sp. was always handled independently of either the modern *C. caespitosa* or any other modern corals. Specimens were first examined by light microscopy; no large exogenous biological material was observed while clays and some recrystallization was apparent as dense, shiny regions similar to secondary calcite (SI Figure S1). Specimens were sonicated for 2.5 hours in deionized water with frequent water changes (every 10-15 minutes) to remove debris and loosely cemented sand. Cleaned fragments were dried at 40°C. After cleaning, sub-fossil coral fragments were only handled in UCLA's dedicated ancient DNA(aDNA) lab under established 'clean' conditions [54,55]. Standard contamination prevention protocols employed included: UV irradiation of the entire lab space before and after each use; only unopened consumables packages were brought into the aDNA lab and boxes were wiped with bleach and UV irradiated before opening and use; PPE always included disposable smocks, hairnets, foot covers, surgical masks, and double-gloving with nitrile gloves; and no modern specimens are ever allowed into the aDNA lab.

aDNA was extracted from eight fragments of cleaned *Cladocora* sp. using a Qiagen PowerSoil kit, per manufacturer's instructions, after four fragments were manually broken to fit into the extraction tubes and four fragments were ground in a mortar and pestle. Each fragment was extracted independently and DNA was eluted in Qiagen solution C6 for four fragments and sterile water for four fragments. Extracted DNA was stored at -80°C.

To compare extracted aDNA quality from *Cladocora* to modern coral skeletons that have seen similar depositional conditions (dead >10 years; stored in coastal sandy sediments near to the surf zone), a colony of *Pocillopora verrucosa* from West Ambae, Vanuatu in co-author JLD's personal collection was cleaned, extracted, and stored as above, with the only difference being that all steps were performed in labs outside of the aDNA lab, using completely different PPE, and on different days from when sub-fossil *Cladocora* sp. specimens were handled.

Prior to sample shipment for library preparation and sequencing, aliquots of all extracted DNA were analyzed by Qubit and TapeStation to assess DNA quantity and quality (SI Table S4). *Cladocora* sp. aDNA was pooled according to grinding and elution buffer, yielding four fossil coral DNA samples in total which were shipped on ice. *P. verrucosa* extracted DNA was not sent for sequencing.

Pooled aDNA was prepared into libraries via the "Spotlight" single stranded library preparation method Santa Cruz Reaction (SCR) optimized specifically for ancient (i.e., degraded) DNA [56], using Illumina P5 and P7 adapters, followed by Qubit and fragment analyzer assessment, and then sequenced on a NextSeq v2.5 - 150 cycles, mid-output - at the UC Santa Cruz Paleogenomics Laboratory. Forward and reverse paired-end reads were imported together to Geneious Prime software for assembly and alignment. Paired reads were trimmed of adapters using the BBDuck plugin with a Kmer value of 27 and a quality score of 20 (99% likelihood of correct base calling). Paired and merged reads from all four pooled aDNA libraries were mapped to mitochondrial genomes from fellow faviids Cyphastrea, Platygyra, and Dipsastraea downloaded from NCBI. Because of the low return rate of reads mapped to faviid mitogenomes, all merged reads from the most promising pooled library (SCS284) were also extracted for further analysis. Mapped reads and all SCS284 merged reads were then separately BLASTed against the NCBI core nucleotide database and best BLAST hit taxonomy was assigned using the taxonomizr package in RStudio.

2.4.3. Species Relationships

Modern *C. caespitosa* CO1 DNA sequences were BLASTed in NCBI and then aligned with all isolates from the same study as the best BLAST hit [57]. These were then aligned with other scleractinian CO1 sequences from the same portion of the gene, as well as a *Nematostella vectensis* (class Anthozoa, order Actiniaria) CO1 sequence as an outgroup. An ancient *Cladocora* CO1 DNA

 doi:10.20944/preprints202507.1343.v1

sequence pulled from the full aDNA dataset was aligned with other scleractinian CO1 sequences from the same portion of the gene - further downstream from the location of the modern *C. caespitosa* sequence, as well as the *Nematostella vectensis* CO1 gene as for the modern alignment. All alignments were performed in T-Coffee [58]. Best model fit was determined using default settings in the ModelFinder tool of IQTree [59] and then trees were predicted in IQTree using 1000 bootstraps; best models based on BIC scores were HKY +F +G4 and K2P +G4 for modern-only upstream and ancient DNA-included downstream CO1 sequences, respectively.

2.5. Compound Specific Stable Isotope Analysis of Amino Acids (CSIA-AA):

2.5.1. Sample Preparation

Tissue from the live coral nubbins collected from Haifa Bay was removed from the skeleton using an airbrush with ultra-pure water, homogenized with an electric homogenizer, and centrifuged three times at 500 xg for 10 min at 4°C to separate host tissue from symbionts. Symbiont pellets were further washed with ultra-pure water after each triplicate centrifugation. Both fractions were freeze-dried before subsequent analysis. Sub-fossil and modern (after tissue removal) coral skeletal fragments were incubated in 3% bleach overnight, then washed in ultra-pure water and sonicated to remove all debris before decalcification for analysis of skeletal organic matter. Approximately 1.5 g of cleaned skeleton from each colony was hydrolyzed in 0.9 M HCl at room temperature until complete decalcification, concentrated via 15 ml Amicon centrifugal filtration units (30kd), and freeze-dried.

2.5.2. CSIA-AA

Amino acid nitrogen and carbon isotopic composition of tissue fractions (modern corals) and skeleton organic matter were determined by gas chromatography/combustion/isotope ratio mass spectrometry (GC/C/IRMS). The acid-hydrolyzed host, symbiont, and skeleton product samples were first derivatized using the EZ:faast kit [24]. Briefly, ~4 mg of the hydrolyzed samples were derivatized with the EZ:faast kit with a slight modification of replacing reagent 6 with dichloromethane as the solvent. Amino acids were separated on a Zebron ZB-50 column (30 m, 0.25 mm, and 0.25 μm) on a Thermo Scientific Trace 1300 Gas Chromatograph using helium as the carrier gas at a constant flow of 1.5 ml/min. For carbon analysis, 1.5 μl was injected in split mode (1:15) at 250°C, while 2 μl was injected in splitless mode at 250°C for nitrogen analysis. The separated amino acids were split on the MicroChannel device into two direction flows: Thermo Scientific ISQ quadruples for amino acid identification and Thermo Scientific Delta-V advantage for C and N isotope analysis. In order to determine the isotopic ratio of carbon and nitrogen, the separated amino acids were combusted in a Thermo scientific GC isolink II at 1000°C for CO2 and N2. Before the sample was run into the Delta-V for N2 analysis, it passed through a cold trap with liquid nitrogen to freeze all other gases. Duplicates for carbon and triplicates for nitrogen were injected from each sample. Stable isotope ratios were expressed in standard δ notation, with the standard for carbon being Vienna PeeDee Belemnite (VPDB) and for nitrogen atmospheric N_2 (air). To account for carbon atoms incorporated during the derivatization process, we followed the correction factor of Docherty et al. [60] for each amino acid. Since the samples are from different time periods all modern samples were applied with Seuss correction to compensate for the changes in modern CO_2 emissions [61]. The trophic position ($TP_{Glu\text{-}Phe}$) was calculated using glutamic acid and phenylalanine with the predefined equation of Chikaraishi et al. [62] and constants from Martinez et al. [24].

3. Results

In 2012-2014, during three season of underwater excavation at Akko Port, within the larger Haifa Bay area (Figure 1; SI Figure 1) eight metal molds were placed on the harbor sea floor at a distance of 20 to 40 meters from the city wall in order to locate the edge of the wharf . During the excavation, stones up to 1.8 m in diameter were moved away to expose the bedrock in three square pits to a depth

 doi:10.20944/preprints202507.1343.v1

of 2.2-2.6 m, while only wharf pavement stones were exposed for cleaning in the remaining squares. Coral colonies and fragments were found *in situ* in the three fully exposed pits. Across pits 1, 2, and 7, a large preserved coral colony 20x20 cm remained affixed to the bedrock, one smaller colony remained connected to the bedrock, and some pottery shards covered with preserved corals were found, respectively [43]. ^{14}C tests of several coral samples dated them to the mid second century to early 1st century BCE during the Hellenistic - Early Roman Period [43]. The preservation of organic fragments, most likely remnants of the polyp (Figure 2A), along with the aragonitic mineralogy and the preservation of the finest skeletal structural elements, such as the nano-granulate structure in rapid accretion deposits (RADs) (Figure 2B,C), confirms that the corals were rapidly buried alive and tightly sealed by a protective layer of sediment.

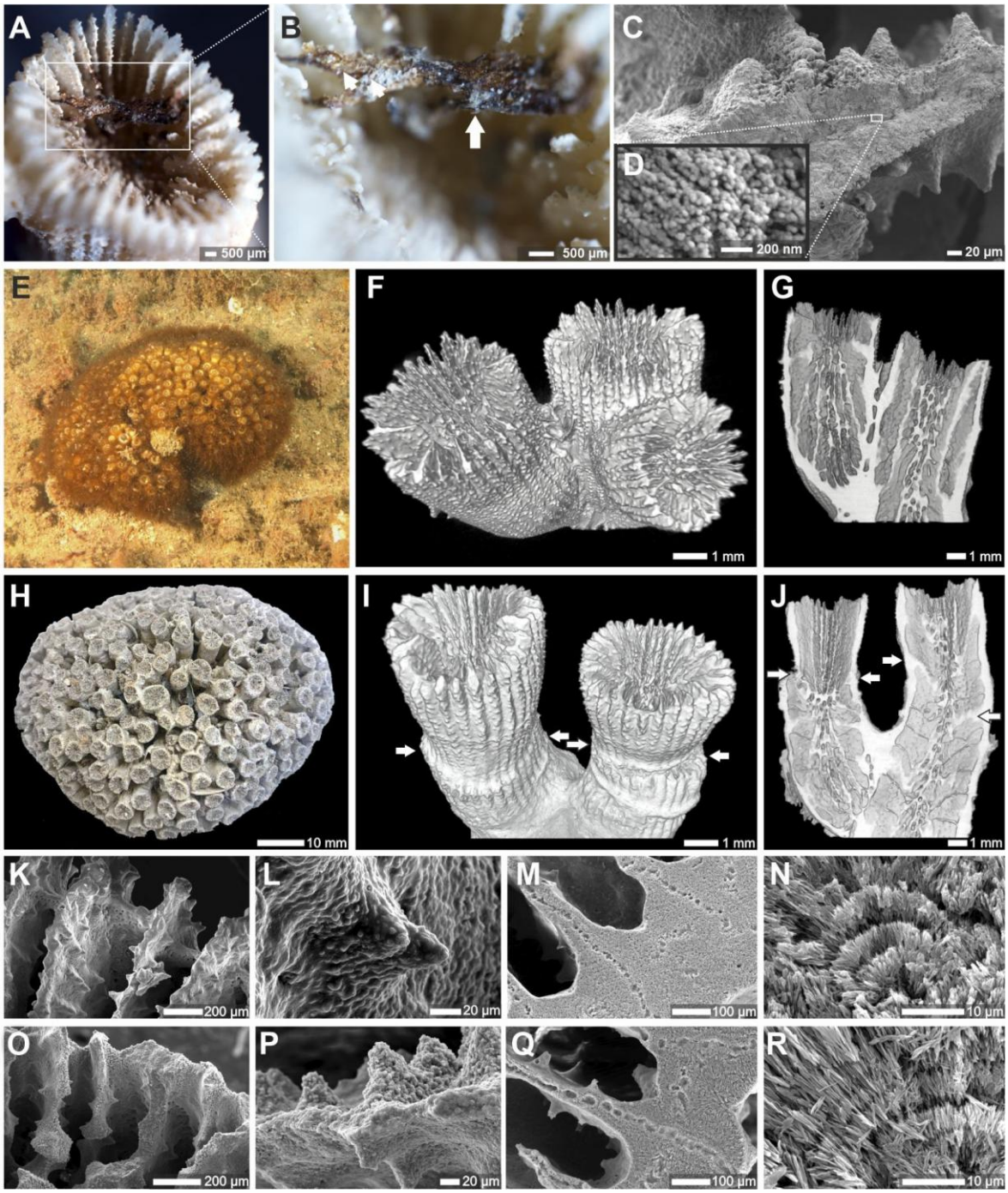

Figure 2. Exceptionally preserved specimens of sub-fossil *Cladocora* display (A,B) dark-brown structures attached to the skeleton and stretched between septa (arrow in B), interpreted as remnants of polyp tissue (examined for aDNA), and (C,D) the nanogranular structure of RADs, which is typically lost even in slightly

 doi:10.20944/preprints202507.1343.v1

diagenetically altered skeletons. Direct morphological comparisons between Recent (E-G–C, K-N) and sub-fossil *Cladocora* (H-J, O-R). The overall colony shape of living (E) and sub-fossil *Cladocora* (H) is shown. Microtomographic reconstructions of modern (F) and sub-fossil (I) corallites are shown along with their virtual sections (G, J, respectively). SEM micrographs show the distal view of calices and the septal faces in both modern (K,L) and sub-fossil (O,P) specimens as well as etched transverse sections of septa and wall of modern (M,N) and sub-fossil (Q,R) specimens.

3.1. Morphology:

The almost identical skeletal structure, from the colony level to the micrometer scale, between the sub-fossil coral and the modern *Cladocora caespitosa* suggests that the sub-fossil coral represents the same taxon (Figure 2). For both specimens, small clumped colonies are composed of tubular, compact, upward facing corallites, each several mm in diameter, with their own distinct corallite wall (i.e., phaceloid) (Figure 2E, H). Microtomographic reconstructions of modern and sub-fossil corallites, along with their virtual sections (Figure 2 F-G, I-J, respectively), reveal identical internal organization in both specimens. Interestingly, some calices of sub-fossil Cladocora show clear constrictions known as rejuvenescence (arrows in Figure 2 I,J). SEM micrographs of the distal view of calices show well-developed septal granulations on the septal faces in both Recent (Figure 2K,L) and sub-fossil (Figure 2O,P) specimens. Etched transverse sections of septa and wall show an identical microstructural organization in Recent (Figure 2M,N) and sub-fossil (Figure 2Q,R) skeletons. The mid-septal zone consists of closely spaced rapid accretion deposits (RADs), which are also visible as part of the wall (the so-called trabeculotheca). Regular, fine-scale banding of thickening deposits (Figure 2N,R) is typical of symbiotic corals [22,63]. The sub-fossil *Cladocora's* septa hexamerally arranged in approximately four cycles are well-preserved, with excellent preservation of RADs and lower inner edges of S1 septa merging with the columella (Figure 2A, C,D), as is observed for modern *C. caespitosa*. To support the visual taxonomic identification, we extracted DNA from both the recent intact *Cladocora* tissue from the Leonid shipwreck and the sub-fossil Akko *Cladocora*'s preserved skeletons with remaining tissue. In addition, we compared these exceptionally-preserved sub-fossil coral remains to living *Cladocora* corals immediately north (Naharia; 10 m specimen for in situ FIRe analyses) and south (Leonid shipwreck; 30 m specimen for in situ FIRe, external DNA sequencing and CSIA-AA analyses) to better understand the underwater environment of Akko Port during the Hellenistic-Roman period.

3.2. DNA Results:

Analyses of cytochrome c oxidase subunit 1 (CO1; Table S1) gene sequences of the modern coral host collected at Haifa Bay from 30 m depth approximately 12 km south of Akko Bay showed 100% match to vouchers for eastern Mediterranean *Cladocora caespitosa* mitochondrial partial COI gene via NCBI nucleotide Blast (accession numbers: MW032500.1-MW032523.1) (Table S2; [57]), confirming the taxonomic assignment based on macro-morphology. The dominant ITS2 (Table S1) symbiont type was identified as *Breviolum psygmophilum* (synonym of *Symbiodinuium psygmophiulm,* clade B2; Table S3).

Ancient DNA extracted from the best quality pooled sub-fossil *Cladocora* sp. sample (SCS284; Figure 3A) was dominated by bacterial sequences, with cnidarians, and more specifically scleractinians, making up 0.3% (non-redundant) and 0.06% (total) BLAST taxonomic assignments of 706,328 merged reads. Of those merged reads, 50-90 mapped to one of the three Faviid mitogenomes used for comparison (Table S4); 10 of these reads mapped to Cyphastraea had best BLAST hits to anthozoan nicotinamide adenine dinucleotide (NADH) subunits and cytochrome oxidase 1 (CO1) (Figure 3C). One read mapped to *Oculina* sp. CO1 (accession no. OQ625380) clusters with the modern Haifa Bay *Cladocora caespitosa* (Figure 3D).

 doi:10.20944/preprints202507.1343.v1

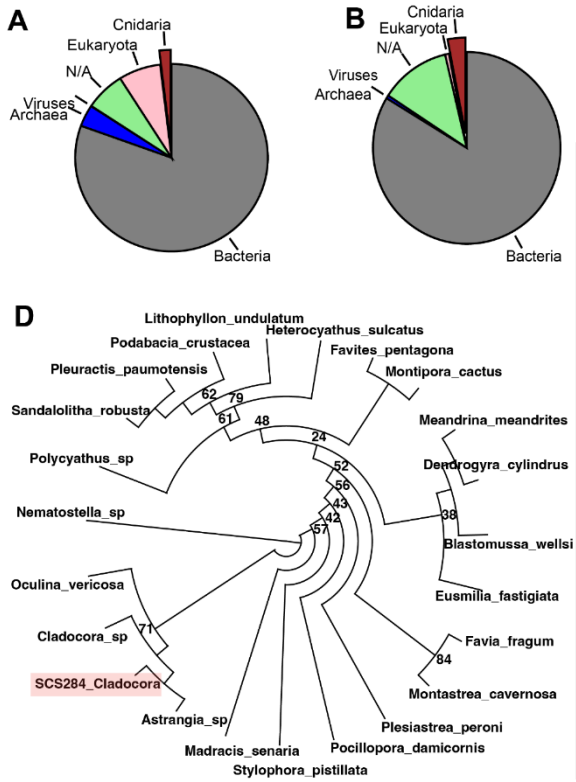

C

SCS284 Merged Read ID	Length (nt)	*Cyphastrea serailia* Mitogenome (NCBI KY094484.1) Blast Location (nt)	Gene	Best BLAST Hit (core_nt)	Best BLAST Hit (core_nt) e-value
NB551675:186:HJN7KAFX3:4:11406:15057:10773 (reversed)	64	7918-7980	NADH dehydrogenase subunit 4 (NAD4)	OQ697534 *Actinia equina* isolate ANT203 NADH dehydrogenase subunit 4 (nad4) gene, partial cds; mitochondrial	2.93E-23
NB551675:186:HJN7KAFX3:2:11304:8715:6026 (reversed)	71	14581-14648	Cytochrome oxidase subunit 1 (CO1)	MG421476 *Anthopleura elegantissima* voucher BCnid2010-036 cytochrome oxidase subunit 1 (COI) gene, partial cds; mitochondrial	4.61E-27
NB551675:186:HJN7KAFX3:3:21401:10047:5289	54	14580-14619	Cytochrome oxidase subunit 1 (CO1)	MG421476 *Anthopleura elegantissima* voucher BCnid2010-036 cytochrome oxidase subunit 1 (COI) gene, partial cds; mitochondrial	7.53E-18
NB551675:186:HJN7KAFX3:3:21505:3259:8310 (reversed)	91	9828-9910	12S ribosomal RNA (mitochondrial)	OQ357273 *Anthopleura handi* isolate NY26 voucher in situ collection small subunit ribosomal RNA gene, partial sequence; mitochondrial	5.37E-38
NB551675:186:HJN7KAFX3:1:11107:20525:3907	53	9543-9589	12S ribosomal RNA (mitochondrial)	OQ357275 *Anthopleura handi* isolate NY30 voucher in situ collection small subunit ribosomal RNA gene, partial sequence; mitochondrial	2.59E-17
NB551675:186:HJN7KAFX3:1:11309:1353:13967 (reversed)	101	11980-12080	Cytochrome oxidase subunit 2 (COX2)	NC030274 *Anthopleura midori* mitochondrion, complete genome	7.96E-42
NB551675:186:HJN7KAFX3:3:11501:1880:5621 (reversed)	106	14825-14928	Cytochrome oxidase subunit 1 (CO1)	NC066051 *Anthopleura xanthogrammica* voucher 2021-05-AX-P01 mitochondrion, complete genome	3.06E-46
NB551675:186:HJN7KAFX3:2:11212:14419:4892 (reversed)	92	9207-9290	12S ribosomal RNA (mitochondrial)	NC066051 *Anthopleura xanthogrammica* voucher 2021-05-AX-P01 mitochondrion, complete genome	4.29E-39
NB551675:186:HJN7KAFX3:3:21405:8605:18582 (reversed)	67	3186-3251	NADH dehydrogenase subunit 1 (NAD1)	OQ697006 *Cladocora* sp. CM-2023 isolate ANT181 NADH dehydrogenase subunit 1 (nad1) gene, partial cds; mitochondrial	6.91E-25
NB551675:186:HJN7KAFX3:3:21511:10869:19680 (reversed)	89	14991-15079	Cytochrome oxidase subunit 1 (CO1)	OQ625380 *Oculina robusta* isolate ANT197 cytochrome c oxidase subunit I (COX1) gene, partial cds; mitochondrial	6.70E-37

Figure 3. aDNA. Scleractinians represent 0.3% and 0.06% of non-redundant (A) and total (B) assigned BLAST hits to all merged reads from the sub-fossil *Cladocora* sp. extraction with the highest number of alignments to three faviid mitogenomes (sample SCS284) and that were over 100 nucleotides in length were BLASTed against the NCBI core nucleotide database with an expect score threshold of e^{-20}; phylum Cnidaria is highlighted within super-kingdom Eukaryota. Ten of 90 merged reads from SCS284 mapped to the *Cyphastrea serialia* mitogenome and had best BLAST hits to cnidarian genes in the NCBI core_nt database (C). One merged SCS284 read mapped and BLASTed to the cnidarian CO1 gene, highlighted in (C); this read clusters with DNA from modern *Cladocora* sp., *Oculina vericosa*, and *Astrangia* sp. (D).

3.3. Photophysiology

Photophysiological measurements of modern *C. caespitosa* growing in Haifa Bay at 10 and 30 m (Naharia and Leonid shipwreck, respectively; Figure 1, SI Figure S2), and therefore different light intensities, show that the connectivity parameter, p, a measure of photoprotection (energy transference between photosystems II and I) and the functional absorption of light, $\boldsymbol{\sigma}_{PSII}$ (a measure of efficiency) did not differ between the two depths ($p > 0.05$; Kruskal-Wallis; SI Figure S3A, B). However, total photosynthetic efficiency (F_v/F_m) was significantly lower in 10 m corals and maximum photosynthetic yield (P_{max}) was significantly lower in 30 m corals (p = 6.182e-08, 1.909e-06; Kruskal-Wallis; respectively Figure 4A, B).

 doi:10.20944/preprints202507.1343.v1

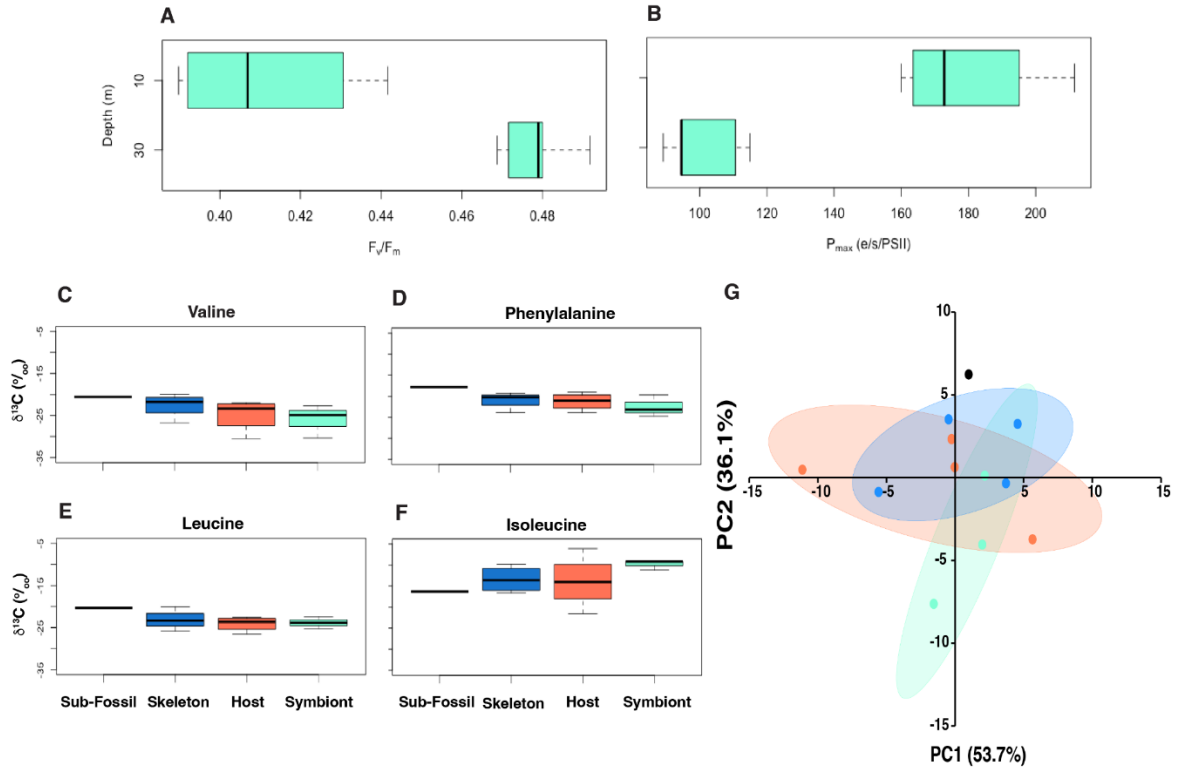

Figure 4. Photophysiology and carbon-transfer. Significantly higher in situ Fv/Fm and lower Pmax were observed in modern C. caespitosa growing at deeper depths (30 m) in the eastern Mediterranean (A, B). Corrected carbon CSIA-AA (C-F). PCA of four essential amino acids (valine, phenylalanine, leucine, and isoleucine) in C. caespitosa host, symbiont, and skeleton, with symbol coloration following that in C-F (G).

3.4. CSIA-AA

Carbon CSIA-AA analysis of four essential AA (valine, leucine, isoleucine, and phenylalanine) indicates that there is no significant difference between the carbon isotopic signature of the host, symbiont, and skeleton of the contemporary Cladocora (PERMANOVA monte-carlo p=0.53, Figure 4G) indicating resource sharing between the coral host and its symbionts. The sub-fossil coral skeleton $\delta^{13}C$ of 3 out of 4 of the essential AA is at least 2‰ higher than all the contemporary compartments (Figure 4 C-F).

Similarly to carbon CSIA-AA analysis, the nitrogen CSIA-AA shows no significant difference between the host, symbiont, and skeleton of the contemporary Cladocora (PERMANOVA monte-carlo p=0.66, Fig-5). However, the sub-fossil coral skeleton $\delta^{15}N$ values of individual amino acids are higher than the contemporary ones by an average of 2-13‰ (Fig-5A-I) except for threonine and isoleucine, which fall within their range. Interestingly, the highest difference (>13‰) is observed in source AA phenylalanine (Figure 5G) which is not affected by trophic discrimination in the food web. There is also no significant difference in the trophic position ($TP_{Glu\text{-}Phe}$) between the host, symbionts, and skeleton of the contemporary coral, and the sub-fossil coral $TP_{Glu\text{-}Phe}$ skeleton is similar to the contemporary one (Figure 5K).

 doi:10.20944/preprints202507.1343.v1

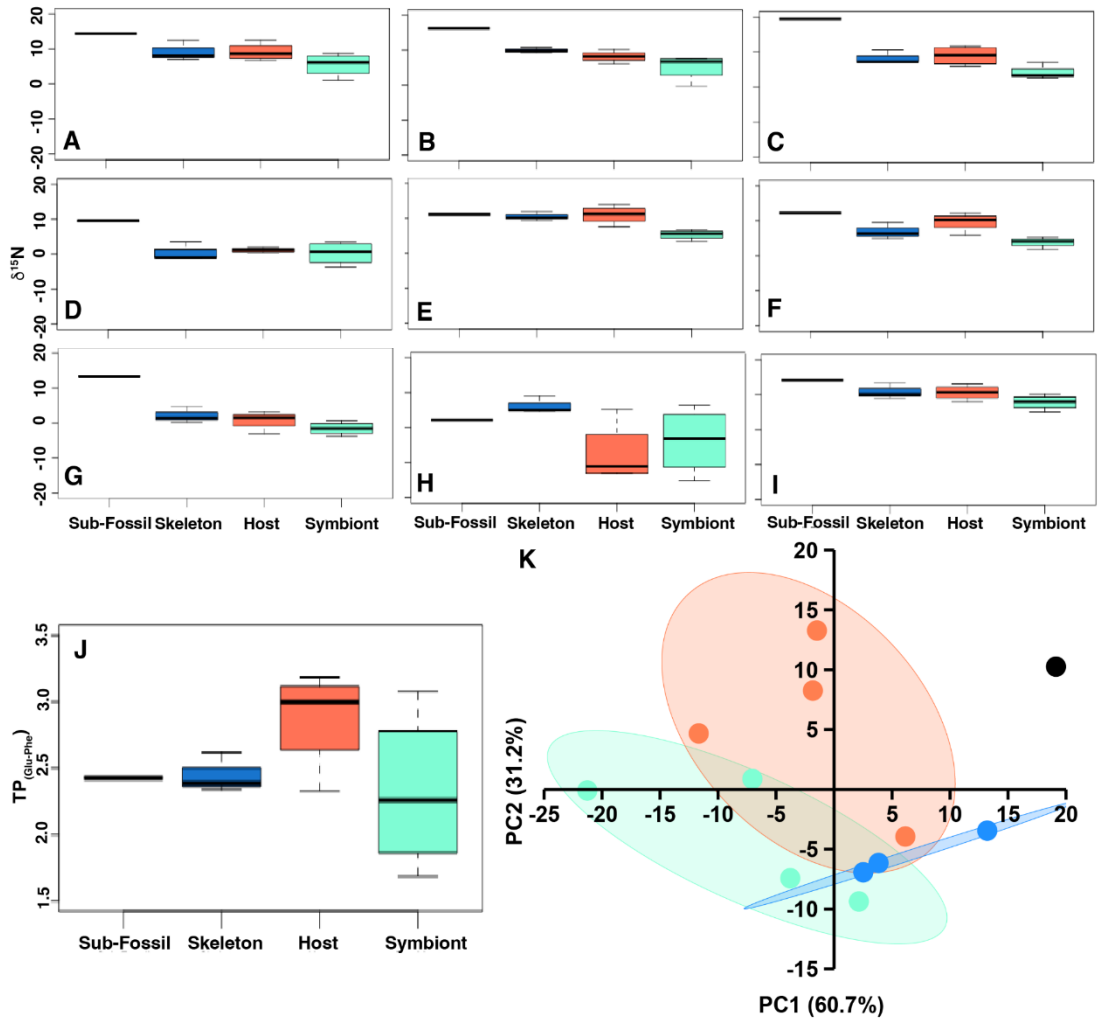

Figure 5. Nitrogen CSIA-AA of host, symbiont and skeleton, and calculated trophic position (TPGlu-Phe) (A-I) Nitrogen isotopic values of nine amino acids (alanine, aspartic acid, glutamic acid, glycine, isoleucine, leucine, phenylalanine, threonine, and valine, respectively). (J) Trophic position of each compartment calculated from $\delta^{15}N_{(Glu\text{-}Phe)}$. (J) PCA of nine amino acids in A-I.

4. Discussion

The Mediterranean Sea is recognized as a long term hotspot of biodiversity, shaped by geological events, climatic fluctuations, and its limited connection to the Atlantic Ocean [64,65]. The region harbors a diverse array of temperate and subtropical species, along with a significant number of endemics [66]. Extensive coral reef systems thrived in the Mediterranean Sea during warmer geological periods, as part of the ancient Tethys more than 200 million years ago [67,68]; however, a major shift in salinity at the end of the Miocene (e.g. six million years ago), termed the Messinian salinity crisis [69] resulted in the near-complete loss of zooxanthellate corals and the disappearance of established shallow-water coral reefs [70]. The sudden opening of Gibraltar filled the Mediterranean again 5.5 million years ago, introducing new scleractinian species to the region [71]. In the present day, shallow rocky seabeds are predominantly covered by frondose algae, while long-lived, filter-feeding organisms prevail in light-deprived benthic communities [72]. The scleractinian coral diversity of the Mediterranean today is relatively low, with 37 representatives [73] compared with over 700 species in the Caribbean and Indo-Pacific, [5].

 doi:10.20944/preprints202507.1343.v1

Since the Messinian crisis, the colonial coral *Cladocora caespitosa* (Linnaeus, 1767; family Cladocoridae) is the only remnant of ancient Mediterranean reefs, resembling tropical reef-builders in its ability to form reef-like structures named "reef banks" [31,74]. Ancient dead banks of *C. caespitosa* (dated from around 2500–3000 yr ago) are known from the coasts of Tunisia and Corsica (central Mediterranean) [75]. While it was abundant during the warmer Pleistocene, still forming reef-like structures [46], modern distribution of this taxon has declined dramatically in the eastern Mediterranean while retaining a fairly abundant presence in the central-western Mediterranean (mainly found near the Tunisian coast, Aegean Sea, Spain, France and Croatia [5,29,31,76–78], from shallow waters to depths of about 50m [32,79], on both hard and soft bottoms [80]. *C. caespitosa* forms small-sized globose to hemispherical colonies ranging from a few hundred polyps to larger banks [76,81], typically of compact arrangements of separated polyps that retain relatively short corallite walls [5], as observed in both the modern and sub-fossil corals examined here (Figure 2). However, *C. caespitosa* colonies can grow as extended and diffuse corallites under extremely low flow conditions ([82]; SI Figure S4). The frequency for smaller colonies may result from high mortality rates or fragmentation due to climate changes [83]. It is a slow-growing coral (2.55 ± 0.79 mm year–1 [32]), and is differentiated from other *Cladocora* taxa both by its upward-only facing polyps and its limited geographic distribution [5,84]. Hence, macro and micro-morphology, as well as DNA sequencing (SI Table S2D) supports identification of the modern *Cladocora* examined here as *C. caespitosa. C. caespitosa* is abundant in the Mediterranean between the surface and 50 m [46,85], the sub-fossil *Cladocora* likely grew at <5 m depth [43], and shallower depths are typically sites of higher flow and elevated temperature. The compact clustering of the sub-fossil *Cladocora* colonies' polyps suggests that they grew in a higher flow environment (Figure 2D,G versus SI Figure S4; [82]). Additionally, the presence of calicular constrictions known as rejuvenescence suggests that this colony survived a past stressor event (Figure 2 I, J) [86]. The ancient specimen's excellent preservation is evidenced in the nano-granular structure of the septa (Figure 2), also observed in rapid accretion deposits of modern coral skeletons collected live [1]. Both macro- and microstructure of the sub-fossil *Cladocora* adhere to descriptions for modern *C. caespitosa*. The intact microstructure and appearance of tissue, combined with evidence of rapid encasement in sediment, support its use in molecular analyses.

Ancient DNA (aDNA) sequencing, along with macro- and micromorphology (Figure 2), supports the sub-fossil *Cladocora* specimen's identification and highlights the increasing role that aDNA analysis can play in historical ecological understanding [87], particularly when species preservation is sufficient. For invertebrates, this can be made particularly difficult by the lack of tissue occlusion in the mineral; however, it is not without precedent as aDNA has been sequenced from ornamental mollusk shells and allowed taxonomic identification [88,89]. It is not surprising that the majority of the sequences from even the best quality aDNA extraction in the present study are off-target (Figure 3A, B). In other aDNA studies, as little as <10% of the mapped reads have been aligned to target nuclear and mitochondrial genomes [90,91], including in the original validation of the library preparation method used here [56], with much of the remaining reads mapping to microbial DNA even when steps are taken to remove microbial DNA accepting sacrificial loss of target DNA as well [92].

Of the two species of *Cladocora* found in the Mediterranean, *C. caespitosa* is the only one with documented photosymbiotic ability [80]. Its plasticity in its ability to shift between heterotrophy and autotrophy for fixed carbon acquisition is often related to strong seasonal variability in light availability [93,94], water motion as waves and currents, type of substrata, and seafloor morphology [29,31,32]. Highly variable physiology and morphology, and unresolved genetic relationships of the Favidae family, have left genus *Cladocora* - and many other taxa in the family - grouped loosely together and considered 'problematic' in terms of classification [95]. However, recent study supports a close phylogenetic relationship between *Oculina patagonica* and *Cladocora caespitosa*, suggesting their placement within the same family, and potentially even the same genus [96]. This variability and unstable phylogenetic classification, combined with its relative scarcity in the eastern Mediterranean, has precluded its previous utility in reconstructing past shallow water ecology in the Levant.

 doi:10.20944/preprints202507.1343.v1

However, the regular, fine-scale banding of thickening deposits, typical of symbiotic corals [22,63] observed here both in the modern and sub-fossil coral (Figure 2) suggest that the sub-fossil coral is indeed *C. caespitosa*.

The coral diet appears to have remained remarkably consistent over the past 2000 years, with a high trophic position (TP) indicating a significant reliance on heterotrophic feeding (here ~2.5 compared with TP ~1 for autotrophy [97]. However, the skeletal δ13C values of sub-fossil *Cladocora* are notably heavier (more positive) than those of their modern counterparts, likely due to differences in light environment [24]. The decoupling between high Fv/Fm and low Pmax observed at the deeper site (Figure 4A-B) suggests that while the photosynthetic apparatus remains functionally efficient, light or downstream metabolic limitations may constrain the overall carbon fixation capacity [98–103]. Under low-light conditions, isotopic discrimination against ^{13}C by Rubisco remains high, favoring the assimilation of ^{12}C and resulting in lighter $\delta^{13}C$ values in the coral skeleton. However, the observation of heavier $\delta^{13}C$ in the sub-fossil samples (Figure 4C-D) indicates that the corals were not experiencing light limitation at the time of growth. Instead, the enriched ^{13}C signature suggests that photosynthetic rates were sufficiently high to reduce isotopic discrimination, consistent with an environment characterized by ample light availability. This interpretation is supported by the paleoenvironmental context, as sub-fossil *Cladocora* colonies likely grew in shallower and less turbid waters, where higher light availability facilitated faster photosynthesis and heavier $\delta^{13}C$ signatures[100–103]. Furthermore, the stable $\delta^{13}C$ values we observe between the two time points ~2000 years apart indicate that the balance between autotrophic and heterotrophic nutrition in the sub-fossil *Cladocora* has remained fairly constant, despite environmental and human-induced changes.

In contrast, significant shifts are evident in nitrogen isotope signals, with nitrogen being heavier in sub-fossil specimens. This difference can be attributed to two interacting factors: (1) historical documents reveal that during the Middle Ages (Crusader period), the city's sewage was discharged directly into the harbor, creating a nutrient-rich environment that is typically turbid; in general, Hellenistic and Roman cities had impressive sanitary systems that collected the sewage and discharged it away from population centers [104–106]. The presence of heavier nitrogen isotope in the sub-fossil coral indicates that sewage was discharged into the port of Akko as early as the Hellenistic period, making anthropogenic land-based nitrogen the primary source for corals then, similar to observations near modern cities experiencing recent rapid growth [107]. (2) The widespread adoption of synthetic fertilizers after 1913, produced using the Haber–Bosch process, which converts atmospheric nitrogen into ammonia, introduced nitrogen with isotopic values close to 0‰. This has contributed to the lowering of nitrogen isotope values observed in modern corals [23,108].

The $\delta^{15}N$ distribution in organic matter preserved within coral skeletons has proven to be a valuable tool for reconstructing historical changes in nitrogen sources. For example, examination of skeletal δ15N in modern Indonesian poritid corals grown between 1970 and 2003 revealed that corals from fertilizer-affected reefs experienced a steady decline in bulk $\delta^{15}N$ values, from +10.7‰ to + 3.5‰, reflecting increased use of chemical fertilizers with low $\delta^{15}N$ values and a reduction in organic manure application in upstream agricultural fields [109]. In contrast, corals and algae from sewage-affected reefs maintained consistently high bulk $\delta^{15}N$ values (>8‰), underscoring the isotopic difference between chemical fertilizers and organic nitrogen sources such as sewage [109]. While changes in bulk $\delta^{15}N$ in coral can be attributed to changes in their heterotrophic diet, CSIA-AA demonstrates that the coral maintained its trophic position. Furthermore, using the source amino acid phenylalanine, which remains unchanged between TP, we show that the modern corals exhibit a relatively low $\delta^{15}N$ value averaging 0.3‰, aligning with the isotopic signature of the Haber–Bosch process. Conversely, sub-fossil corals, unaffected by synthetic fertilizers, show much heavier $\delta^{15}N$-phenylalanine values, approximately 13‰, resembling those found in sewage-affected environments.

 doi:10.20944/preprints202507.1343.v1

The remarkably high degree of preservation of the sub-fossil *C. caespitosa* - intact microstructures and lack of secondary infillings [110] and the fact that the corals were found below the Hellenistic quay was likely due to a rapid burial process [43]. This burial was possibly triggered by a sudden singular sedimentation event caused by anthropogenic activity, such as the foundation of the harbor, that could cause changes in sediment movement or other changes inside the harbor, as supported by archaeological evidence from the region [43]. Additionally, the discovery of multiple *Cladocora* specimens in all the pits that reached the bedrock during the excavation in Akko suggests a historically larger population. In contrast, no *Cladocora* colonies were documented by the surveys of the Morris Kahn Marine Research Station Long Term Ecological Research program (MKMRS LTER; established in 2014—https://med-lter.haifa.ac il/index.php/en/data-base) conducted along the Israeli coasts which indicate a limited distribution with only two known sites harboring a few colonies each.

The discrepancy between historical and current *Cladocora* population, along with the rapid increase in temperature in the eastern Mediterranean [36] suggests that the population reduction may be related to climate change, pollution, and habitat destruction [111]. Persistence of the species in the eastern Mediterranean today therefore suggests that the population was able to adapt, migrate locally, or repopulate from sites further west [50], or some combination of these. The species may continue to use these mechanisms today in response to the effects of Anthropocene climate change. Minimal reef accretion observed in the eastern Mediterranean over the past several thousand years precludes coring for a fine-resolution temporal study of ecosystem shifts as performed in tropical locations [e.g., [112]]; however, the present study provides important timepoints and geographic locations of comparison in an anthropogenically dynamic environment [113]. Further, the present and similar recent studies comparing between data sets from modern organisms and ancient environments, utilizing private collections and newly collected specimens as well as emerging sources in museum-held collections and government- and NGO-directed cultural excavations may also serve as lessons for furthering our understanding of how other coral taxa will meet climate change impacts [e.g., [107,114,115].

5. Conclusions

Through the interdisciplinary comparison of a 2000 year old coral skeleton with modern taxonomic brethren, we propose a framework of the ecological structure of Akko port ~2000 years ago. At that time, shallow water *Cladocora caespitosa*, a zooxanthellate stony coral, settled on appropriately hard substrates at a relatively shallow depth with sufficient water flow to promote the formation of compact colonies. Our results suggest that these corals thrived in a high-flow, nutrient-rich, and turbid environment; however, despite the turbidity, light availability was adequate to sustain efficient photosynthesis, likely due to the colony's position in water shallow enough to allow sufficient light penetration. The colonies possibly survived one or more stressor events. These corals were mixotrophic, like their modern counterparts, and occupied a similar trophic position, with port water clear enough to support photosymbiosis supplemented by phyto- and zooplankton communities, possibly supported by nutrient-rich effluent from the city of Akko similar to anthropogenic coastal nutrient loading observed today in urbanizing coastal systems [108,116,117]. A sudden catastrophic event entombed the colony studied here, leaving it akin to a hard drive containing much and varied data about the past ecology of the port. Because *C. caespitosa* colonies are rarely found in the eastern Mediterranean today under similar conditions, the present comparison shows how temperate stony corals, and the structures they provide, respond (adapt, migrate, or die out) to local physical conditions. Similar ecological reconstructions in other locations will also require very well-preserved specimens at both the microscopic (e.g., mineralogical for geochemical analyses) and macroscopic scales as well as modern local analogs for holistic comparison.

Supplementary Materials: The following supporting information can be downloaded at the website of this paper posted on Preprints.org., Figure S1: Location of the excavation pit from Akko Port; Figure S2. Modern *C. caespitosa* colonies; Figure S3. Photophysiology parameters; Figure S4. Morphological plasticity of *C. caespitosa* ;

 doi:10.20944/preprints202507.1343.v1

Table S1. Modern DNA primer information; Table S2. Modern *C. caespitosa* host DNA sequence; Table S3. Modern *C. caespitosa* symbiont DNA sequence; Table S4. Ancient DNA sequencing metrics

Author Contributions: Conceptualization, T.M. and J.S.; methodology, T.M., J.S., J.D., S.M. and J.S.; formal analysis, T.M., J.S., J.D., S.M. and J.S.; resources, T.M.; writing— T.M., J.S., J.D., S.M. and J.S,; writing—review and editing, T.M., J.S., J.D., S.M. and J.S; visualization, T.M., J.S., J.D., S.M. and J.S; funding acquisition, T.M. All authors have read and agreed to the published version of the manuscript.

Funding: This research was funded by the Ministry of Innovation, Science and Technology, Israel (Grant # 0002193) TM.

Institutional Review Board Statement: Not applicable.

Informed Consent Statement: Not applicable.

Data Availability Statement: All other raw data and code are available on Github: https://github.com/talimass/Cladocora.git

Acknowledgments: We thank the Scientific Diving Programs and DSOs at the University of Haifa and Israeli Antiquities Authority. We thank Mollie Cassatt-Johnstone, Samuel Sacco, and Beth Shapiro at the US Santa Cruz Paleogenomics Laboratory for consultation and aDNA sequencing. The authors have reviewed and edited the output and take full responsibility for the content of this publication."

Conflicts of Interest: The authors declare no conflicts of interest.

References

1. Drake, J.L.; Mass, T.; Stolarski, J.; Von Euw, S.; van de Schootbrugge, B.; Falkowski, P.G. How Corals Made Rocks through the Ages. Glob. Chang. Biol. 2020, 26, 31–53.
2. Knowlton, N.; Brainard, R.E.; Fisher, R.; Moews, M.; Plaisance, L.; Caley, M.J. Coral Reef Biodiversity. In Life in the World's Oceans; Wiley-Blackwell: Oxford, UK, 2010; pp. 65–78 ISBN 9781444325508.
3. Rocha, L.A.; Bowen, B.W. Speciation in Coral-reef Fishes. J. Fish Biol. 2008, 72, 1101–1121.
4. Mumby, P.J.; Broad, K.; Brumbaugh, D.R.; Dahlgren, C.P.; Harborne, A.R.; Hastings, A.; Holmes, K.E.; Kappel, C.V.; Micheli, F.; Sanchirico, J.N. Coral Reef Habitats as Surrogates of Species, Ecological Functions, and Ecosystem Services: Coral Reef Habitats as Surrogates. Conserv. Biol. 2008, 22, 941–951.
5. Veron, J.E.N. Corals of the World; Australian Institute of Marine Sciences: Townsville, 2000;.
6. Malik, A.; Einbinder, S.; Martinez, S.; Tchernov, D.; Haviv, S.; Almuly, R.; Zaslansky, P.; Polishchuk, I.; Pokroy, B.; Stolarski, J.; et al. Molecular and Skeletal Fingerprints of Scleractinian Coral Biomineralization: From the Sea Surface to Mesophotic Depths. Acta Biomater. 2021, 120, 263–276.
7. Bellworthy, J.; Pardo, R.; Scucchia, F.; Zaslansky, P.; Goodbody-Gringley, G.; Mass, T. Physiological and Morphological Plasticity in *Stylophora Pistillata* Larvae from Eilat, Israel, to Shallow and Mesophotic Light Conditions. iScience 2023, 26, 106969.
8. Scucchia, F.; Wong, K.; Zaslansky, P.; Putnam, H.M.; Goodbody-Gringley, G.; Mass, T. Morphological and Genetic Mechanisms Underlying the Plasticity of the Coral *Porites Astreoides* across Depths in Bermuda. J. Struct. Biol. 2023, 215, 108036.
9. Goodbody-Gringley, G.; Waletich, J. Morphological Plasticity of the Depth Generalist Coral, *Montastraea Cavernosa*, on Mesophotic Reefs in Bermuda. Ecology 2018, 99, 1688–1690.
10. Mass, T.; Brickner, I.; Hendy, E.; Genin, A. Enduring Physiological and Reproductive Benefits of Enhanced Flow for a Stony Coral. Limnol. Oceanogr. 2011, 56, 2176–2188.
11. Mass, T.; Genin, A. Environmental versus Intrinsic Determination of Colony Symmetry in the Coral *Pocillopora Verrucosa*. Mar. Ecol. Prog. Ser. 2008, 369, 131–137.
12. Helmuth, B.; Sebens, K. The Influence of Colony Morphology and Orientation to Flow on Particle Capture by the Scleractinian Coral *Agaricia Agaricites* (Linnaeus). J. Exp. Mar. Bio. Ecol. 1993, 165, 251.
13. Patterson, M.R. A Mass-Transfer Explanation of Metabolic Scaling Relations in Some Aquatic Invertebrates and Algae. Science 1992, 255, 1421–1423.

 doi:10.20944/preprints202507.1343.v1

14. Stanley, G.D., Jr The Evolution of Modern Corals and Their Early History. Earth Sci. Rev. 2003, 60, 195–225.
15. Thompson, D.M. Environmental Records from Coral Skeletons: A Decade of Novel Insights and Innovation. Wiley Interdiscip. Rev. Clim. Change 2022, 13, doi:10.1002/wcc.745.
16. DeLong, K.L.; Quinn, T.M.; Taylor, F.W.; Shen, C.-C.; Lin, K. Improving Coral-Base Paleoclimate Reconstructions by Replicating 350years of Coral Sr/Ca Variations. Palaeogeogr. Palaeoclimatol. Palaeoecol. 2013, 373, 6–24.
17. Trotter, J.; Montagna, P.; McCulloch, M.; Silenzi, S.; Reynaud, S.; Mortimer, G.; Martin, S.; Ferrier-Pagès, C.; Gattuso, J.-P.; Rodolfo-Metalpa, R. Quantifying the pH "vital Effect" in the Temperate Zooxanthellate Coral Cladocora Caespitosa: Validation of the Boron Seawater pH Proxy. Earth Planet. Sci. Lett. 2011, 303, 163–173.
18. Gothmann, A.M.; Stolarski, J.; Adkins, J.F.; Schoene, B.; Dennis, K.J.; Schrag, D.P.; Mazur, M.; Bender, M.L. Fossil Corals as an Archive of Secular Variations in Seawater Chemistry since the Mesozoic. Geochim. Cosmochim. Acta 2015, 160, 188–208.
19. Muscatine, L.; Goiran, C.; Land, L.; Jaubert, J.; Cuif, J.-P.; Allemand, D. Stable Isotopes (delta13C and delta15N) of Organic Matrix from Coral Skeleton. Proc. Natl. Acad. Sci. U. S. A. 2005, 102, 1525–1530.
20. Wang, X.T.; Sigman, D.M.; Cohen, A.L.; Sinclair, D.J.; Sherrell, R.M.; Weigand, M.A.; Erler, D.V.; Ren, H. Isotopic Composition of Skeleton-Bound Organic Nitrogen in Reef-Building Symbiotic Corals: A New Method and Proxy Evaluation at Bermuda. Geochim. Cosmochim. Acta 2015, 148, 179–190.
21. Jung, J.; Zoppe, S.F.; Söte, T.; Moretti, S.; Duprey, N.N.; Foreman, A.D.; Wald, T.; Vonhof, H.; Haug, G.H.; Sigman, D.M.; et al. Coral Photosymbiosis on Mid-Devonian Reefs. Nature 2024, 636, 647–653.
22. Frankowiak, K.; Wang, X.T.; Sigman, D.M.; Gothmann, A.M.; Kitahara, M.V.; Mazur, M.; Meibom, A.; Stolarski, J. Photosymbiosis and the Expansion of Shallow-Water Corals. Sci. Adv. 2016, 2, e1601122.
23. Wang, X.T.; Sigman, D.M.; Cohen, A.L.; Sinclair, D.J.; Sherrell, R.M.; Cobb, K.M.; Erler, D.V.; Stolarski, J.; Kitahara, M.V.; Ren, H. Influence of Open Ocean Nitrogen Supply on the Skeletal δ15N of Modern Shallow-Water Scleractinian Corals. Earth Planet. Sci. Lett. 2016, 441, 125–132.
24. Martinez, S.; Kolodny, Y.; Shemesh, E.; Scucchia, F.; Nevo, R.; Levin-Zaidman, S.; Paltiel, Y.; Keren, N.; Tchernov, D.; Mass, T. Energy Sources of the Depth-Generalist Mixotrophic Coral *Stylophora Pistillata*. Front Mar Sci 2020, 7, 988.
25. Kast, E.R.; Griffiths, M.L.; Kim, S.L.; Rao, Z.C.; Shimada, K.; Becker, M.A.; Maisch, H.M.; Eagle, R.A.; Clarke, C.A.; Neumann, A.N.; et al. Cenozoic Megatooth Sharks Occupied Extremely High Trophic Positions. Sci. Adv. 2022, 8, eabl6529.
26. Kast, E.R.; Stolper, D.A.; Auderset, A.; Higgins, J.A.; Ren, H.; Wang, X.T.; Martínez-García, A.; Haug, G.H.; Sigman, D.M. Nitrogen Isotope Evidence for Expanded Ocean Suboxia in the Early Cenozoic. Science 2019, 364, 386–389.
27. Tornabene, C.; Martindale, R.C.; Wang, X.T.; Schaller, M.F. Detecting Photosymbiosis in Fossil Scleractinian Corals. Sci. Rep. 2017, 7, 9465.
28. Wang, X.T.; Wang, Y.; Auderset, A.; Sigman, D.M.; Ren, H.; Martínez-García, A.; Haug, G.H.; Su, Z.; Zhang, Y.G.; Rasmussen, B.; et al. Oceanic Nutrient Rise and the Late Miocene Inception of Pacific Oxygen-Deficient Zones. Proc. Natl. Acad. Sci. U. S. A. 2022, 119, e2204986119.
29. Zibrowius, H. Les Scléractiniaires de La Méditerranée et de l'Atlantique Nord-Oriental. Mem. Inst. Oceanogr. Monaco 1980.
30. Aguirre, J.; Jiménez, A.P. Fossil Analogues of Present-Day *Cladocora Caespitosa* Coral Banks: Sedimentary Setting, Dwelling Community, and Taphonomy (Late Pliocene, W Mediterranean). Coral Reefs 1998, 17, 203–213.
31. Kružić, P.; Žuljević, A.; Nikolić, V. Spawning of the Colonial Coral *Cladocora Caespitosa* (Anthozoa, Scleractinia) in the Southern Adriatic Sea. Coral Reefs 2008, 27, 337–341.
32. Kersting, D.-K.; Linares, C. Cladocora Caespitosa Bioconstructions in the Columbretes Islands Marine Reserve (Spain, NW Mediterranean): Distribution, Size Structure and Growth: *Cladocora Caespitosa* bioconstructions in the Columbretes Islands Marine Reserve. Mar. Ecol. 2012, 33, 427–436.

 doi:10.20944/preprints202507.1343.v1

33. Peirano, A.; Kružić, P. Growth Comparison between Ligurian and Adriatic Samples of the Coral Cladocora Caespitosa: First Results. Biologia marina mediterranea 2004, 11, 166–168.
34. Silenzi, S.; Bard, E.; Montagna, P.; Antonioli, F. Isotopic and Elemental Records in a Non-Tropical Coral (*Cladocora Caespiosa*): Discovery of a New High-Resolution Climate Archive for the Mediterranean Sea. Glob. Planet. Change 2005, 49, 94–120.
35. Nantet, E. The Rise of the Tonnage in the Hellenistic Period. In Sailing from polis to empire: Ships in the eastern Mediterranean during the Hellenistic period; Nantet, E., Ed.; OpenBook: Adelaide, SA, Australia, 2020; pp. 75–89.
36. Sisma-Ventura, G.; Yam, R.; Shemesh, A. Recent Unprecedented Warming and Oligotrophy of the Eastern Mediterranean Sea within the Last Millennium. Geophys. Res. Lett. 2014, 41, 5158–5166.
37. Ozer, T.; Gertman, I.; Kress, N.; Silverman, J.; Herut, B. Interannual Thermohaline (1979–2014) and Nutrient (2002–2014) Dynamics in the Levantine Surface and Intermediate Water Masses, SE Mediterranean Sea. Glob. Planet. Change 2017, 151, 60–67.
38. Grainger, J.D. The Syrian Wars; Brill, 2010;.
39. Ben-Yosef, D. Akko Bay: Hinterland of Phoenician Commercial City during the Persian Period. In In the Hill-Country, and in the Shephelah, and in the Arabah, Studies and Researches Presented to Adam Zertal in the Thirtieth Anniversary of the Manasseh Hill-Country Survey; Bar, S., Ed.; Jerusalem, 2008; pp. 271–290.
40. Sharvit, J.; Planer, D.; Buxton, B.; Hale, J.; Barkai, O. Akko, Underwater Excavation; Hadashot Arkeologiot, Excavation and Surveys in Israel, 2023;.
41. Makhouly, N.; Johns, C.N. Guide to Acre; Government of Palestine Department of Antiquities: Jerusalem, 1946;.
42. Linder, E.; Raban, A. From the Diary of the Acre Expedition. Bimtzuloth-Yam 1965, 7, 23–27.
43. Sharvit, J.; Buxton, B.; Hale, J.R.; Ratzlaff, A. The Hellenistic-Early Roman Harbour of Akko: Preliminary Finds from Archaeological Excavations at the Foot of the Southeastern Seawall at Akko, 2008-2014. In Under the Mediterranean I: Studies in Maritime Archaeology; Demesticha, S., Blue, L., Eds.; Sidestone Press: Leiden, Netherlands, 2021; pp. 163–180.
44. Pietraszek, A. The Submerged Hellenistic to Early Roman Harbor at Akko: A Geoarchaeological Approach, University of Haifa, 2018.
45. Peirano, A.; Morri, C.; Bianchi, C.N. Skeleton Growth and Density Pattern of the Temperate, Zooxanthellate Scleractinian *Cladocora Caespitosa* from the Ligurian Sea (NW Mediterranean). Mar. Ecol. Prog. Ser. 1999, 185, 195–201.
46. Peirano, A.; Morri, C.; Bianchi, C.N.; Rodolfo-Metalpa, R. Biomass, Carbonate Standing Stock and Production of the Mediterranean coral *Cladocora Caespitosa* (L.). Facies 2001, 44, 75–80.
47. Gorbunov, M.Y.; Falkowski, P.G. Using Chlorophyll Fluorescence Kinetics to Determine Photosynthesis in Aquatic Ecosystems. Limnol. Oceanogr. 2021, 66, 1–13.
48. Carpenter, G.E.; Chequer, A.D.; Weber, S.; Mass, T.; Goodbody-Gringley, G. Light and Photoacclimatization Drive Distinct Differences between Shallow and Mesophotic Coral Communities. Ecosphere 2022, 13, doi:10.1002/ecs2.4200.
49. Schöne, B.R.; Dunca, E.; Fiebig, J.; Pfeiffer, M. Mutvei's Solution: An Ideal Agent for Resolving Microgrowth Structures of Biogenic Carbonates. Palaeogeogr. Palaeoclimatol. Palaeoecol. 2005, 228, 149–166.
50. Martinez, S.; Bellworthy, J.; Ferrier-Pagès, C.; Mass, T. Selection of Mesophotic Habitats by *Oculina Patagonica* in the Eastern Mediterranean Sea Following Global Warming. Sci. Rep. 2021, 11, 18134.
51. Folmer, O.; Black, M.; Hoeh, W.; Lutz, R.; Vrijenhoek, R. DNA Primers for Amplification of Mitochondrial Cytochrome c Oxidase Subunit I from Diverse Metazoan Invertebrates. Mol. Mar. Biol. Biotechnol. 1994, 3, 294–299.
52. Arif, C.; Daniels, C.; Bayer, T.; Banguera-Hinestroza, E.; Barbrook, A.; Howe, C.J.; LaJeunesse, T.C.; Voolstra, C.R. Assessing Symbiodinium Diversity in Scleractinian Corals via next-Generation Sequencing-Based Genotyping of the ITS2 rDNA Region. Mol. Ecol. 2014, 23, 4418–4433.

 doi:10.20944/preprints202507.1343.v1

53. Hume, B.C.C.; Smith, E.G.; Ziegler, M.; Warrington, H.J.M.; Burt, J.A.; LaJeunesse, T.C.; Wiedenmann, J.; Voolstra, C.R. SymPortal: A Novel Analytical Framework and Platform for Coral Algal Symbiont next-Generation Sequencing ITS2 Profiling. Mol. Ecol. Resour. 2019, 19, 1063–1080.
54. Orlando, L.; Allaby, R.; Skoglund, P.; Der Sarkissian, C.; Stockhammer, P.W.; Ávila-Arcos, M.C.; Fu, Q.; Krause, J.; Willerslev, E.; Stone, A.C.; et al. Ancient DNA Analysis. Nat. Rev. Methods Primers 2021, 1, doi:10.1038/s43586-020-00011-0.
55. Knapp, M.; Clarke, A.C.; Horsburgh, K.A.; Matisoo-Smith, E.A. Setting the Stage - Building and Working in an Ancient DNA Laboratory. Ann. Anat. 2012, 194, 3–6.
56. Kapp, J.D.; Green, R.E.; Shapiro, B. A Fast and Efficient Single-Stranded Genomic Library Preparation Method Optimized for Ancient DNA. Journal of Heredity 2021, 112, 241–249.
57. López-Márquez, V.; Lozano-Martín, C.; Hadjioannou, L.; Acevedo, I.; Templado, J.; Jimenez, C.; Taviani, M.; Machordom, A. Asexual Reproduction in Bad Times? The Case of Cladocora Caespitosa in the Eastern Mediterranean Sea. Coral Reefs 2021, 40, 663–677.
58. Di Tommaso, P.; Moretti, S.; Xenarios, I.; Orobitg, M.; Montanyola, A.; Chang, J.-M.; Taly, J.-F.; Notredame, C. T-Coffee: A Web Server for the Multiple Sequence Alignment of Protein and RNA Sequences Using Structural Information and Homology Extension. Nucleic Acids Res. 2011, 39, W13–W17.
59. Kalyaanamoorthy, S.; Minh, B.Q.; Wong, T.K.F.; von Haeseler, A.; Jermiin, L.S. ModelFinder: Fast Model Selection for Accurate Phylogenetic Estimates. Nat. Methods 2017, 14, 587–589.
60. Docherty, G.; Jones, V.; Evershed, R.P. Practical and Theoretical Considerations in the Gas Chromatography/combustion/isotope Ratio Mass Spectrometry delta(13)C Analysis of Small Polyfunctional Compounds: Practical and Theoretical Considerations in GC/C/IRMS. Rapid Commun. Mass Spectrom. 2001, 15, 730–738.
61. Francey, R.J.; Allison, C.E.; Etheridge, D.M.; Trudinger, C.M.; Enting, I.G.; Leuenberger, M.; Langenfelds, R.L.; Michel, E.; Steele, L.P. A 1000-Year High Precision Record of delta13C in Atmospheric CO2. Tellus B Chem. Phys. Meteorol. 1999, 51, 170–193.
62. Chikaraishi, Y.; Ogawa, N.O.; Kashiyama, Y.; Takano, Y.; Suga, H.; Tomitani, A.; Miyashita, H.; Kitazato, H.; Ohkouchi, N. Determination of Aquatic Food-Web Structure Based on Compound-Specific Nitrogen Isotopic Composition of Amino Acids. Limnol. Oceanogr. Methods 2009, 7, 740–750.
63. Frankowiak, K.; Kret, S.; Mazur, M.; Meibom, A.; Kitahara, M.V.; Stolarski, J. Fine-Scale Skeletal Banding Can Distinguish Symbiotic from Asymbiotic Species among Modern and Fossil Scleractinian Corals. PLoS One 2016, 11, e0147066.
64. Boudouresque, C.-F. Marine Biodiversity in the Mediterranean: Status of Species, Populations and Communities. Travaux scientifiques du Parc national de Port-Cros 2004, 20, 97–146.
65. Templado, J. Future Trends of Mediterranean Biodiversity. In The Mediterranean Sea; Springer Netherlands: Dordrecht, 2014; pp. 479–498 ISBN 9789400767034.
66. Coll, M.; Piroddi, C.; Steenbeek, J.; Kaschner, K.; Ben Rais Lasram, F.; Aguzzi, J.; Ballesteros, E.; Bianchi, C.N.; Corbera, J.; Dailianis, T.; et al. The Biodiversity of the Mediterranean Sea: Estimates, Patterns, and Threats. PLoS One 2010, 5, e11842.
67. Cristino J. Dabrio Mateu Esteban The Coral Reef of Nijar, Messinian (uppermost Miocene), Almeria Province, S. E. Spain. J. Sediment. Res. 1981, 51, doi:10.1306/212f7cca-2b24-11d7-8648000102c1865d.
68. Pomar, L. Reef Geometries, Erosion Surfaces and High-frequency Sea-level Changes, Upper Miocene Reef Complex, Mallorca, Spain. Sedimentology 1991, 38, 243–269.
69. Martín, J.; Braga, J.C. Messinian Events in the Sorbas Basin in Southeastern Spain and Their Implications in the Recent History of the Mediterranean. Sediment. Geol. 1994, 90, 257–268.
70. Vertino, A.; Stolarski, J.; Bosellini, F.R.; Taviani, M. Mediterranean Corals through Time: From Miocene to Present. In The Mediterranean Sea; Springer Netherlands: Dordrecht, 2014; pp. 257–274 ISBN 9789400767034.
71. Freiwald, A. 5 Messinian Salinity Crisis: What Happened to Cold-Water Corals? In Mediterranean Cold-Water Corals: Past, Present and Future; Springer International Publishing: Cham, 2019; pp. 47–50 ISBN 9783319916071.

 doi:10.20944/preprints202507.1343.v1

72. Zabala, M.; Ballesteros, E. Surface-Dependent Strategies and Energy Flux in Benthic Marine Communities Or, Why Corals Do Not Exist in the Mediterranean. Sci. Mar. 1989, 53, 3–17.
73. Stambler, N. Life in the Mediterranean Sea: A Look at Habitat Changes; Nova Science Publishers, Inc, 2012;.
74. Schuhmacher, H.; Zibrowius, H. What Is Hermatypic?: A Redefinition of Ecological Groups in Corals and Other Organisms. Coral Reefs 1985, 4, 1–9.
75. Laborel, J. Marine Biogenic Constructions in the Mediterranean, a Review. Sci. Rep. Port-Cros natl. Park 1987, 13, 97–126.
76. Peirano, A.; Morri, C.; Mastronuzzi, G.A.; Bianchi, C.N. The Coral *Cladocora Caespitosa* (Anthozoa, Scleractinia) as a Biotherm Builder in the Mediterranean Sea: A Short Review. Memorie Descrittive della Carta geologica d'Italia 1994, 52, 59–74.
77. Kersting, D.K.; Teixidó, N.; Linares, C. Recruitment and Mortality of the Temperate Coral *Cladocora Caespitosa*: Implications for the Recovery of Endangered Populations. Coral Reefs 2014, 33, 403–407.
78. Kružić, P.; Sršen, P.; Benković, L. The Impact of Seawater Temperature on Coral Growth Parameters of the Colonial Coral *Cladocora Caespitosa* (Anthozoa, Scleractinia) in the Eastern Adriatic Sea. Facies 2012, 58, 477–491.
79. Morri, C.; Peirano, A.; Bianchi, C.N.; Sassarini, M. Present Day Bioconstructions of the Hard Coral, *Cladocora Caespitosa* (L.)(Anthozoa, Scleractinia), in the Eastern Ligurian Sea (NW Mediterranean). Biol. Mar. Mediterr. 1994.
80. Schiller, C. Ecology of the Symbiotic Coral Cladocora Caespitosa (L.) (faviidae, Scleractinia) in the Bay of Piran (Adriatic Sea): I. Distribution and Biometry. Mar. Ecol. 1993, 14, 205–219.
81. Kružić, P.; Požar-Domac, A. Banks of the Coral *Cladocora Caespitosa* (Anthozoa, Scleractinia) in the Adriatic Sea. Coral Reefs 2003, 22, 536–536.
82. Sanna, G.; Büscher, J.V.; Freiwald, A. Cold-Water Coral Framework Architecture Is Selectively Shaped by Bottom Current Flow. Coral Reefs 2023, 42, 483–495.
83. Zunino, S.; Pitacco, V.; Mavrič, B.; Orlando-Bonaca, M.; Kružić, P.; Lipej, L. The Ecology of the Mediterranean Stony Coral *Cladocora Caespitosa* (Linnaeus, 1767) in the Gulf of Trieste (northern Adriatic Sea): A 30-Year Long Story. Mar. Biol. Res. 2018, 14, 307–320.
84. Baron-Szabo, R.C. Geographic and Stratigraphic Distributions of the Caribbean Species of Cladocora (Scleractinia, Faviidae). Facies 2005, 51, 185–196.
85. Tremblay, P.; Ferrier-Pagès, C.; Maguer, J.F.; Rottier, C.; Legendre, L.; Grover, R. Controlling Effects of Irradiance and Heterotrophy on Carbon Translocation in the Temperate Coral Cladocora Caespitosa. PLoS One 2012, 7, e44672.
86. Kersting, D.K.; Linares, C. Living Evidence of a Fossil Survival Strategy Raises Hope for Warming-Affected Corals. Sci. Adv. 2019, 5, eaax2950.
87. Del Carmen Gomez Cabrera, M.; Young, J.M.; Roff, G.; Staples, T.; Ortiz, J.C.; Pandolfi, J.M.; Cooper, A. Broadening the Taxonomic Scope of Coral Reef Palaeoecological Studies Using Ancient DNA. Mol. Ecol. 2019, 28, 2636–2652.
88. Martin-Roy, R.; Thyrring, J.; Mata, X.; Bangsgaard, P.; Bennike, O.; Christiansen, G.; Funder, S.; Gotfredsen, A.B.; Gregersen, K.M.; Hansen, C.H.; et al. Advancing Responsible Genomic Analyses of Ancient Mollusc Shells. PLoS One 2024, 19, e0302646.
89. Der Sarkissian, C.; Möller, P.; Hofman, C.A.; Ilsøe, P.; Rick, T.C.; Schiøtte, T.; Sørensen, M.V.; Dalén, L.; Orlando, L. Unveiling the Ecological Applications of Ancient DNA from Mollusk Shells. Front. Ecol. Evol. 2020, 8, doi:10.3389/fevo.2020.00037.
90. Harney, É.; Cheronet, O.; Fernandes, D.M.; Sirak, K.; Mah, M.; Bernardos, R.; Pinhasi A Minimally Destructive Protocol for DNA Extraction from Ancient Teeth. Genome research 2021, 31, 472–483.
91. Straube, N.; Lyra, M.L.; Paijmans, J.L.A.; Preick, M.; Basler, N.; Penner, J.; Rödel, M.-O.; Westbury, M.V.; Haddad, C.F.B.; Barlow, A.; et al. Successful Application of Ancient DNA Extraction and Library Construction Protocols to Museum Wet Collection Specimens. Mol. Ecol. Resour. 2021, 21, 2299–2315.
92. Korlević, P.; Gerber, T.; Gansauge, M.-T.; Hajdinjak, M.; Nagel, S.; Aximu-Petri, A.; Meyer, M. Reducing Microbial and Human Contamination in DNA Extractions from Ancient Bones and Teeth. Biotechniques 2015, 59, 87–93.

 doi:10.20944/preprints202507.1343.v1

93. Ferrier-Pagès, C.; Gevaert, F.; Reynaud, S.; Beraud, E.; Menu, D.; Janquin, M.-A.; Cocito, S.; Peirano, A. In Situ Assessment of the Daily Primary Production of the Temperate Symbiotic Coral *Cladocora Caespitosa*. Limnol. Oceanogr. 2013, 58, 1409–1418.
94. Hoogenboom, M.; Rodolfo-Metalpa, R.; Ferrier-Pagès, C. Co-Variation between Autotrophy and Heterotrophy in the Mediterranean Coral *Cladocora Caespitosa*. Journal of Experimental Biology 2010, 213, 2399–2409.
95. Huang, D.; Licuanan, W.Y.; Baird, A.H.; Fukami, H. Cleaning up the "Bigmessidae": Molecular Phylogeny of Scleractinian Corals from Faviidae, Merulinidae, Pectiniidae and Trachyphylliidae. BMC Evol. Biol. 2011, 11, 37.
96. Addamo, A.M.; Modrell, M.S.; Taviani, M.; Machordom, A. Unravelling the Relationships among Madrepora Linnaeus, 1758, Oculina Lamark, 1816 and Cladocora Ehrenberg, 1834 (Cnidaria: Anthozoa: Scleractinia). Invertebr. Syst. 2024, 38, doi:10.1071/IS23027.
97. Ferrier-Pagès, C.; Martinez, S.; Grover, R.; Cybulski, J.; Shemesh, E.; Tchernov, D. Tracing the Trophic Plasticity of the Coral-Dinoflagellate Symbiosis Using Amino Acid Compound-Specific Stable Isotope Analysis. Microorganisms 2021, 9, 182.
98. Omata, T.; Suzuki, A.; Sato, T.; Minoshima, K.; Nomaru, E.; Murakami, A.; Murayama, S.; Kawahata, H.; Maruyama, T. Effect of Photosynthetic Light Dosage on Carbon Isotope Composition in the Coral Skeleton: Long-term Culture of Porites Spp: EFFECT OF LIGHT ONδ13C IN THE CORAL SKELETON. J. Geophys. Res. 2008, 113, doi:10.1029/2007jg000431.
99. Prada, F.; Yam, R.; Levy, O.; Caroselli, E.; Falini, G.; Dubinsky, Z.; Goffredo, S.; Shemesh, A. Kinetic and Metabolic Isotope Effects in Zooxanthellate and Non-Zooxanthellate Mediterranean Corals along a Wide Latitudinal Gradient. Front. Mar. Sci. 2019, 6, doi:10.3389/fmars.2019.00522.
100. Einbinder, S.; Mass, T.; Brokovich, E.; Dubinsky, Z.; Erez, J.; Tchernov, D. Changes in Morphology and Diet of the Coral *Styophora Pistillata* along a Depth Gradient. Mar. Ecol. Prog. Ser. 2009, 381, 167–174.
101. Heikoop, J.M.; Dunn, J.J.; Risk, M.J.; Tomascik, T.; Schwarcz, H.P.; Sandeman, I.M.; Sammarco, P.W. δ ^{15}N and δ ^{13}C of Coral Tissue Show Significant Inter-Reef Variation. Coral Reefs-Journal of the International Society for Reef Studies 2000, 19, 189–193.
102. Muscatine, L.; Porter, J.W.; Kaplan, I.R. Resource Partitioning by Reef Corals as Determined from Stable Isotope Composition: I. δ ^{13}C of Zooxanthellae and Animal Tissue vs Depth. Mar. Biol. 1989, 100, 185–193.
103. Nahon, S.; Richoux, N.B.; Kolasinski, J.; Desmalades, M.; Ferrier Pages, C.; Lecellier, G.; Planes, S.; Berteaux Lecellier, V. Spatial and Temporal Variations in Stable Carbon (δ^{13}C) and Nitrogen (δ^{15}N) Isotopic Composition of Symbiotic Scleractinian Corals. PLoS One 2013, 8, e81247.
104. Yannopoulos, S.; Yapijakis, C.; Kaiafa-Saropoulou, A.; Antoniou, G.; Angelakis, A.N. History of Sanitation and Hygiene Technologies in the Hellenic World. J. Water Sanit. Hyg. Dev. 2017, 7, 163–180.
105. Angelakis, A.N.; Capodaglio, A.G.; Dialynas, E.G. Wastewater Management: From Ancient Greece to Modern Times and Future. Water (Basel) 2022, 15, 43.
106. Barkai, O.; Jaijel, R.; Sharvit, J.; Goodman-Tchernov, B. The Location of the Coastline During the Late Roman and Early Byzantine Periods. Skyllis 6–13.
107. Duprey, N.N.; Wang, T.X.; Kim, T.; Cybulski, J.D.; Vonhof, H.B.; Crutzen, P.J.; Haug, G.H.; Sigman, D.M.; Martínez-García, A.; Baker, D.M. Megacity Development and the Demise of Coastal Coral Communities: Evidence from Coral Skeleton δ^{15}N Records in the Pearl River Estuary. Glob. Chang. Biol. 2020, 26, 1338–1353.
108. Rico-Esenaro, S.D.; de Jesús Adolfo Tortolero-Langarica, J.; Iglesias-Prieto, R.; Carricart-Ganivet, J.P. The δ^{15}N in Orbicella Faveolata Organic Matter Reveals Anthropogenic Impact by Sewage Inputs in a Mexican Caribbean Coral Reef Lagoon. Environ. Sci. Pollut. Res. Int. 2023, 30, 118872–118880.
109. Marion, G.S.; Dunbar, R.B.; Mucciarone, D.A.; Kremer, J.N.; Lansing, J.S.; Arthawiguna, A. Coral Skeletal δ^{15}N Reveals Isotopic Traces of an Agricultural Revolution. Mar. Pollut. Bull. 2005, 50, 931–944.
110. Nothdurft, L.D.; Webb, G.E. Earliest Diagenesis in Scleractinian Coral Skeletons: Implications for Palaeoclimate-Sensitive Geochemical Archives. Facies 2009, 55, 161–201.
111. Chefaoui, R.M.; Casado-Amezúa, P.; Templado, J. Environmental Drivers of Distribution and Reef Development of the Mediterranean Coral Cladocora Caespitosa. Coral Reefs 2017, 36, 1195–1209.

 doi:10.20944/preprints202507.1343.v1

112. Cramer, K.L.; O'Dea, A.; Carpenter, C.; Norris, R.D. A 3000 Year Record of Caribbean Reef Urchin Communities Reveals Causes and Consequences of Long-Term Decline in Diadema Antillarum. Ecography (Cop.) 2018, 41, 164–173.
113. McClenachan, L.; Rick, T.; Thurstan, R.H.; Trant, A.; Alagona, P.S.; Alleway, H.K.; Armstrong, C.; Bliege Bird, R.; Rubio-Cisneros, N.T.; Clavero, M.; et al. Global Research Priorities for Historical Ecology to Inform Conservation. Endanger. Species Res. 2024, 54, 285–310.
114. Drake, J.L.; Whitelegge, J.P.; Jacobs, D.K. First Sequencing of Ancient Coral Skeletal Proteins. Sci. Rep. 2020, 10, 19407.
115. Flewellen, A.O. The Biophysical Afterlife of Slavery Signaled through Coral Architectural Stones at Heritage Sites on St. Croix. Am. Antiq. 2024, 89, 591–607.
116. Sherwood, O.A.; Lapointe, B.E.; Risk, M.J.; Jamieson, R.E. Nitrogen Isotopic Records of Terrestrial Pollution Encoded in Floridian and Bahamian Gorgonian Corals. Environ. Sci. Technol. 2010, 44, 874–880.
117. Luu, V.H.; Ryu, Y.; Darling, W.S.; Oleynik, S.; de Putron, S.J.; Cohen, A.L.; Wang, X.T.; Sigman, D.M. Nitrogen Isotope Ratios across the Bermuda Coral Reef: Implications for Coral Nitrogen Sources and the Coral-Bound Nitrogen Isotope Proxy. Front. Mar. Sci. 2025, 12, doi:10.3389/fmars.2025.1554418.